AWARD NUMBER: W81XWH-14-1-0287

TITLE: The HGF/c-MET Axis as a Critical Driver of Resistance to Androgen Suppression in Metastatic Castrate-Resistant Prostate Cancer

PRINCIPAL INVESTIGATOR: Todd M. Morgan

CONTRACTING ORGANIZATION: University of Michigan, Ann Arbor, MI

REPORT DATE: DECEMBER 2018

TYPE OF REPORT: FINAL

PREPARED FOR: U.S. Army Medical Research and Materiel Command
Fort Detrick, Maryland 21702-5012

REPORT DOCUMENTATION PAGE

Form Approved
OMB No. 0704-0188

1. REPORT DATE	2. REPORT TYPE	3. DATES COVERED
DECEMBER 2018	Final report	9/19/2014-9/18/2018

4. TITLE AND SUBTITLE

The HGF/c-MET Axis as a Critical Driver of Resistance to Androgen Suppression in Metastatic Castrate-Resistant Prostate Cancer

5a. CONTRACT NUMBER
W81XWH-14-1-0287

5b. GRANT NUMBER
PC131841

5c. PROGRAM ELEMENT NUMBER

6. AUTHOR(S)
Todd M. Morgan

E-Mail: tomorgan@med.umich.edu

5d. PROJECT NUMBER

5e. TASK NUMBER

5f. WORK UNIT NUMBER

7. PERFORMING ORGANIZATION NAME(S) AND ADDRESS(ES)

THE UNIVERSITY OF MICHIGAN
ANN ARBOR, MI 48109

8. PERFORMING ORGANIZATION REPORT NUMBER

9. SPONSORING / MONITORING AGENCY NAME(S) AND ADDRESS(ES)

U.S. Army Medical Research and Materiel Command
Fort Detrick, Maryland 21702-5012

10. SPONSOR/MONITOR'S ACRONYM(S)

11. SPONSOR/MONITOR'S REPORT NUMBER(S)

12. DISTRIBUTION / AVAILABILITY STATEMENT

Approved for Public Release; Distribution Unlimited

13. SUPPLEMENTARY NOTES

14. ABSTRACT

In this Physician Research Training Award, the primary goal is to elucidate the role of the HGF/c-MET axis in metastatic castration-resistant prostate cancer. During the current funding period, we have confirmed an inverse relationship between MET expression and AR signaling in prostate cancer cell lines. Our data supports negative regulation of MET by AR signaling, and we found that AR signaling inhibition in AR-positive CRPC models increased MET expression and resulted in susceptibility to ligand (HGF) activation. Likewise, our work over the past year showed that MET inhibition was only effective in blocking cancer phenotypes in cells with MET overexpression. Using multiple AR-positive CRPC models, as detailed in the initial proposal, we found that combined MET inhibition and enzalutamide (AR antagonist) treatment was more efficacious than either inhibitor alone. These data support the concept that the MET pathway may be an key mechanism of resistance in men with CRPC who undergo potent androgen signaling inhibition with abiraterone or enzalutamide.

15. SUBJECT TERMS

Prostate cancer, metastasis, androgen deprivation therapy, human growth factor, MET, enzalutamide, abiraterone, cabozantinib, circulating tumor cells, disseminated tumor cells

16. SECURITY CLASSIFICATION OF:			17. LIMITATION OF ABSTRACT	18. NUMBER OF PAGES	19a. NAME OF RESPONSIBLE PERSON
a. REPORT	b. ABSTRACT	c. THIS PAGE			USAMRMC
Unclassified	Unclassified	Unclassified	Unclassified	36	19b. TELEPHONE NUMBER *(include area code)*

Table of Contents

Page

Introduction

In this Physician Research Training Award, the primary goals are both to further my training as a surgeon scientist and to elucidate the role of the HGF/c-MET axis in metastatic castration-resistant prostate cancer. In so doing, the overarching goal is to develop a durable cure of prostate cancer through a deeper understanding of prostate cancer metastasis and mechanisms of therapeutic resistance. The career development component of the award involves training in molecular biology techniques and biomarker discovery, with close mentorship from Drs. Arul Chinnaiyan and Russell Taichman. The primary scientific aims of this grant are to: 1) Define the mechanisms by which the HGF/c-MET axis facilitates proliferation and viability of CRPC cells in vitro, 2) Define the role of the HGF/c-MET axis in supporting resistance to androgen suppression in mCRPC patients with and without next generation anti-androgen therapy, and 3) Identify the mechanisms by which the HGF/c-MET axis emerges as a mediator of acquired resistance to abiraterone therapy.

Keywords

Prostate cancer, metastasis, androgen deprivation therapy, human growth factor, MET, enzalutamide, abiraterone, cabozantinib, circulating tumor cells, disseminated tumor cells

Accomplishments

Major Task 1: *Establish the response to enzalutamide in distinct PCa cell lines and determine the extent to which c-MET inhibition recovers androgen suppression. (months 1-18)*

We confirmed an inverse relationship between MET expression and AR signaling in prostate cancer cell lines. Our data supports negative regulation of MET by AR signaling, and we found that AR signaling inhibition in AR-positive CRPC models increased MET expression and resulted in susceptibility to ligand (HGF) activation. Likewise, our work showed that MET inhibition is only effective in blocking cancer phenotypes in cells with MET overexpression. Using multiple AR-positive CRPC models, as detailed in the initial proposal, we found that combined MET inhibition and enzalutamide (AR antagonist) treatment was more efficacious than either inhibitor alone. These data support the concept that the MET pathway may be a key mechanism of resistance in men with CRPC who undergo potent androgen signaling inhibition with abiraterone or enzalutamide. This suggests potential utility for MET inhibition in select patients with AR therapy resistance and in AR-negative prostate cancer. In addition, our findings suggest that combined AR and MET inhibition in CRPC may be more effective that inhibiting these pathways sequentially.

This work has resulted in a number of publications during the time period of this award:

Patnaik A, Swanson KD, Csizmadia E, Solanki A, Elemento O, Novak J, Thornley TB, **Morgan TM**, Wang, Y, Wang Y, Levantini E, Clohessy JG, Kelly K, Pandolfi PP, Rosenblatt JM, Avigan DE, Ye H, Karp JM, Signoretti S, Balk SP, Cantley LC,: Cabozantinib Eradicates Advanced Murine Prostate Cancer by Activating Anti-Tumor Innate Immunity. *Cancer Discov*, 8: 1158/2159-8290, 2017. PMCID: PM28274958

Roca H, Jones JD, Purica MC, Weidner S, Koh AJ, Kuo R, Wilkinson JE, Wang Y, Daignault-Newton S, Pienta KJ, **Morgan TM**, Keller ET, Nör JE, Shea LD, McCauley LK: Apoptosis-induced CXCL5 accelerates inflammation and growth of prostate tumor metastases in bone. J Clin Invest 128: 248-266, 2018. PM29202471

Jung Y, Cackowski FC, Yumoto K, Decker A, Wang J, Kim J, Lee E, Wang Y, Chung JS, Gursky AM, Krebsbach PH, Pienta KJ, **Morgan TM**, Taichman RS: CXCL12γ Promotes Development of Metastatic Castration Resistant Prostate Cancer by Induction of Cancer Stem Cell and Neuroendocrine Phenotypes. Cancer Res 78: 2026-2039, 2018. PM29431639

Qiao, Y, Feng, FY, Wang, Y, Cao, X, Han, S., Wilder-Romans, K, Keller, ET, Palapattu, GS, Taichman, RS, Alva, AS, Smith, DC, Tomlins, SA, Chinnaiyan, AM, Tomlins, SA, **Morgan, TM**: Mechanistic support for combined MET and AR blockade in castration resistant prostate cancer. Neoplasia 18:1-9, 2016. PMCID: 26806347.

Major Task 1: *Establish the response to enzalutamide in distinct PCa cell lines and determine the extent to which c-MET inhibition recovers androgen suppression. (months 1-18)*

The following 2 subtasks are presented together:

Subtask 1: *Determine cell proliferation, invasion, migration, and expression of AR and HGF/c-MET axis in PCa cell lines*
Subtask 2: *Determine impact of enzalutamide on cell proliferation, invasion, migration, and expression of AR and HGF/c-MET axis in PCa cell lines*

In order to assess the relationship between AR and MET, we performed Western blot analyses and real time PCR to determine their expression in a number of prostate cancer cell lines. These data strongly supported the inverse relationship of AR and MET.

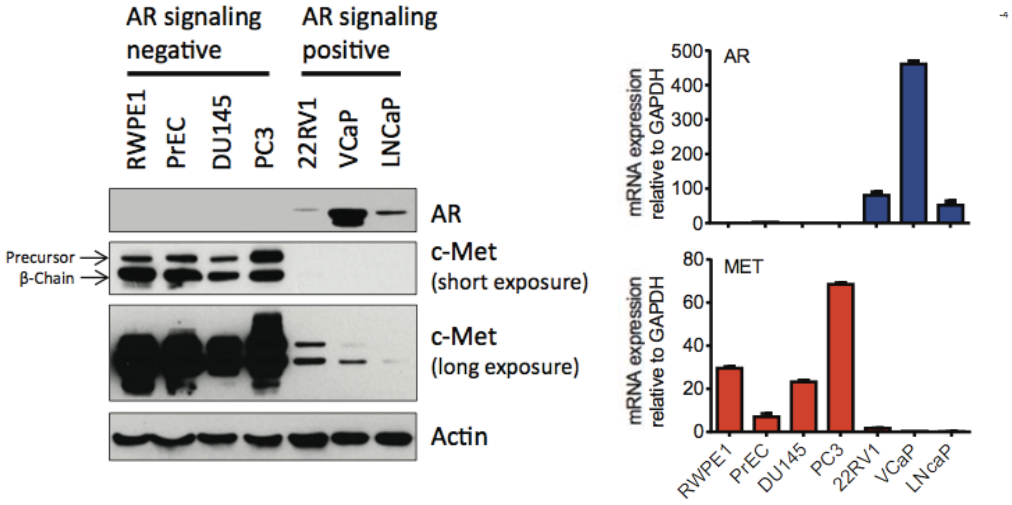

Figure 1: AR and MET expression assessed by Western blot analysis in a series of AR-negative and AR+ prostate cancer cell lines

To further assess MET expression and its correlation with AR expression, we used flow cytometry to sort VCaP cells (AR+/MET^{low}) according to levels of MET expression. We then used real time PCR to compare AR expression in those cells with the highest MET expression with AR expression in those cells with the lowest MET expression. Significant differences in AR expression were present, providing further support for negative regulation of MET by AR signaling.

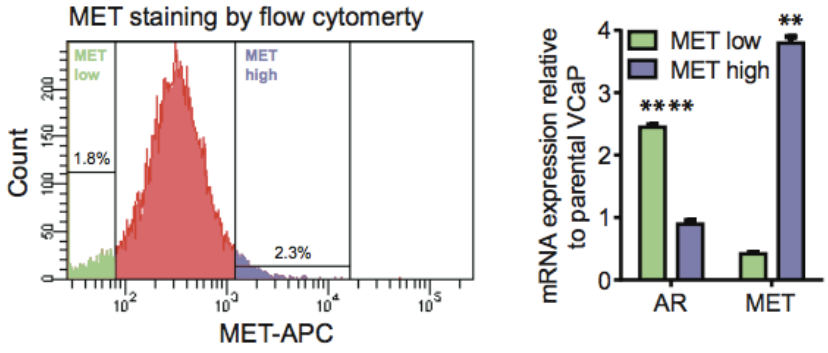

Figure 2: VCaP (AR+/MET-) cells were flow sorted according to the level of MET expression. AR and MET expression was compared by RT-PCR in the MET-low vs. MET-high cells.
Proliferation of LNCaP cells was confirmed to be increased by increasing concentration of DHT and inhibited by enzalutamide.

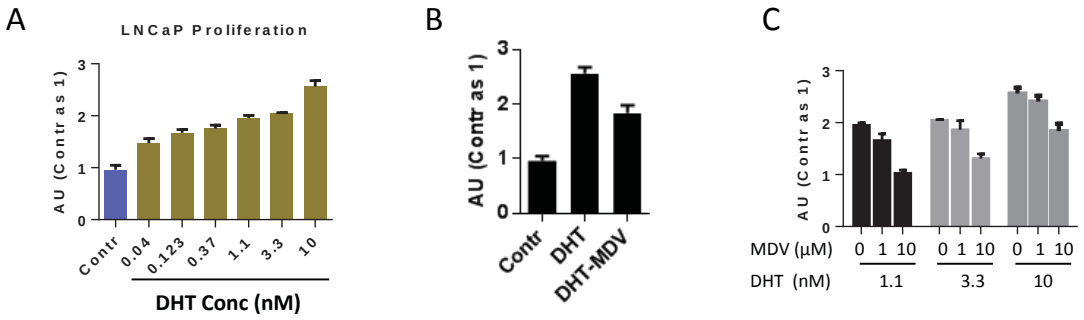

Figure 3: Proliferation of LNCaP cells was assessed with A) varying concentrations of DHT and B) in the setting of DHT + enzalutamide (MDV). C) Enzalutamide inhibited LNCaP proliferation at different doses and in the presence of varying concentrations of DHT.

Proliferation of PC3 (AR-) cells was not impacted by the addition of DHT.

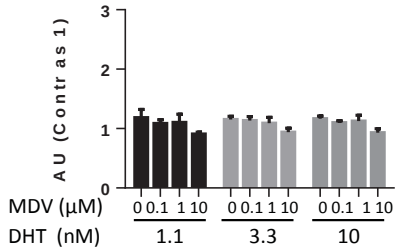

Figure 4: Proliferation of PC3 cells was assessed using varying concentrations of DHT and enzalutamide (MDV), and no significant changes in proliferation were observed.

Additionally, the Figure below shows results of our invasion and migration assays. Both invasion and migration were assessed in the setting of DHT and using DHT + enzalutamide. Invasion and migration of PC3 cells was not impacted by DHT or enzalutamide, as anticipated. LNCaP invasion was increased in the setting of DHT and subsequently inhibited by enzalutamide.

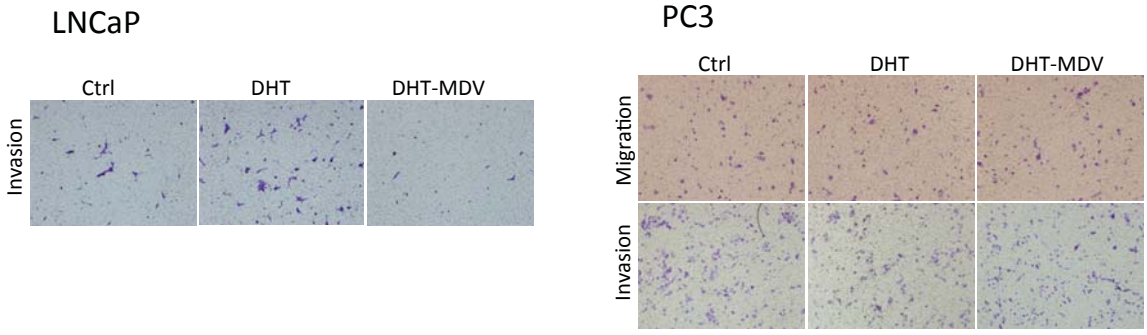

Figure 5: The left panel shows invasion assay results using LNCaP cells and demonstrated the increase in invasiveness associated with DHT, which was subsequently diminished with the addition of enzalutamide (MDV). PC3 cell invasion and migration was unchanged with DHT and with the addition of enzalutamide.

We assessed the impact of enzalutamide on MET expression in VCaP, LNCaP, and LNCaP-AR cells. As shown below, we found that MET expression is increased after exposure to the AR

antagonist enzalutamide and when cells are cultured in charcoal stripped medium (to remove AR hormonal ligands). We elected to use the natural androgen dihydrotestosterone (DHT) rather than the synthetic androgen R1881 and determined that DHT decreases MET expression under charcoal stripped conditions in an enzalutamide sensitive manner.

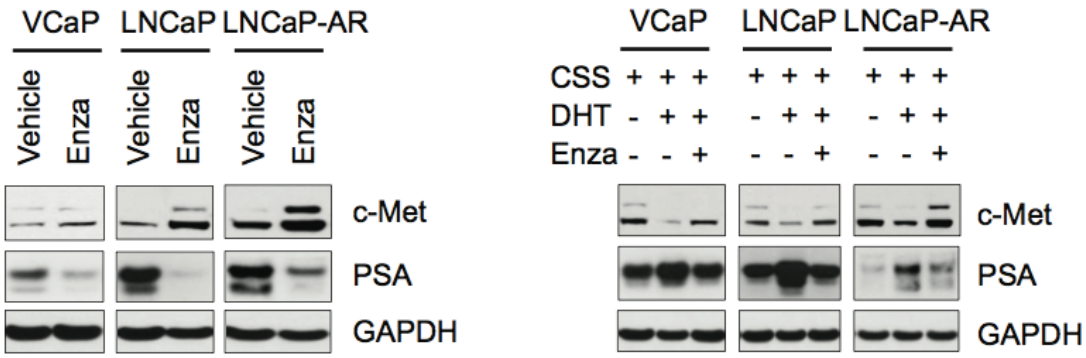

Figure 6: Blockade of androgen signaling increases MET expression *in vitro.*
Left: AR-positive cells (VCaP, LNCaP and LNCaP-AR) were treated with 10μM enzalutamide (Enza), followed by western blot to measure MET and PSA protein levels.
Right: Indicated cells were treated with charcoal stripped serum (CSS) for 48 hours prior to stimulation with DHT (10nM) and enzalutamide treatments for another 24 hours. Expression of indicated proteins were assessed by western blot.

Subtask 3: *Evaluate impact of c-MET/HGF axis inhibition using c-MET siRNA, anti-HGF neutralizing antibody, and exogenous HGF in PCa cell lines*

In this subtask, we sought to credential MET as a potential therapeutic target in AR-negative prostate cancer. The figure below shows that in the presence of HGF, siRNA mediated MET knockdown in PC3 and DU145 cells (AR-/high MET expression) significantly reduced invasion and migration. However, MET knockdown did not affect cell proliferation in PC3 and DU145 cells. Likewise, in the presence of HGF, levels of both p-MET and p-ERK were substantially reduced after MET knockdown in both PC3 and DU145 cells.

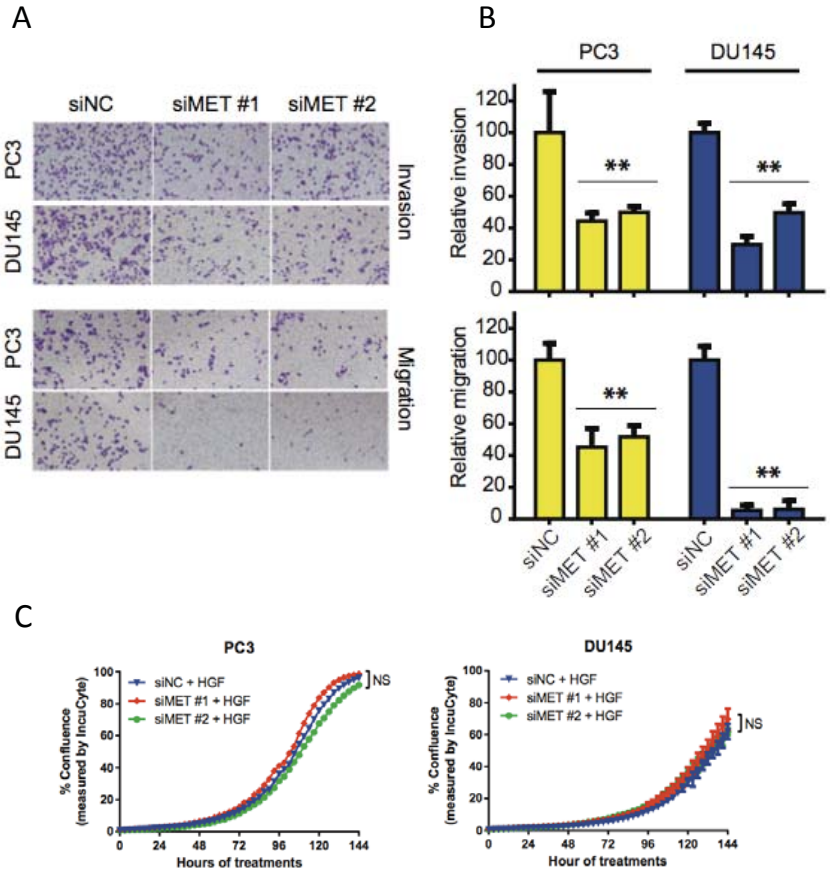

Figure 7: MET/HGF axis promotes invasion in prostate cancer *in vitro*. (**A**) Knockdown of MET in DU145 and PC3 (AR^-) prostate cancer cells. Invasion or migration assays were done in the presence of MET ligand HGF for 24 hours. Representative pictures of crystal violet staining are shown in (**A**), and quantification is shown in (**B**). (**C**) Cell proliferation assays were analyzed by IncuCyte for PC3 and DU145 cells with indicated treatments, and results were shown in percentage of confluence.

We further assessed HGF mediated invasion in both DU145 and PC3 cells in response to cabozantinib and found significant inhibition of invasion.

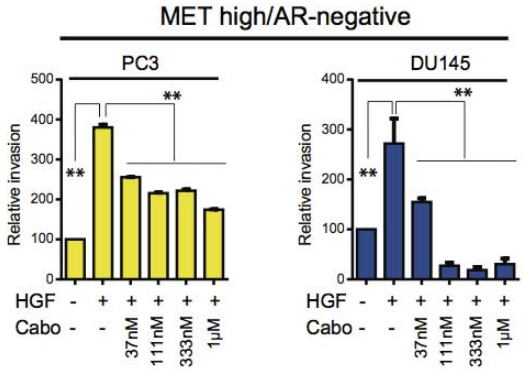

Figure 8: Invasion assays were performed in the presence of HGF and/or various treatment doses of cabozantinib (Cabo) in MET high/AR-negative prostate cancer cells for 24 hours.

In order to see whether there is downregulation of AR when MET is overexpressed, we measured protein levels of AR and MET in stable MET overexpressing LNCaP cells. These results showed that overexpression of MET in AR+ LNCaP cells does not affect endogenous AR protein levels. Thus, regulation of AR and MET appears to be one-directional in AR+ CRPC, with suppression of MET by active AR signaling through possible posttranslational modification.

Figure 9: AR and MET expression assessed by Western blot analysis in LNCaP cells overexpressing MET compared to vector controls. No change in AR expression is observed with MET overexpression.

To further understand the impact of HGF/MET signaling on cell invasion in MET+ and MET- CRPC cell lines, LNCaP and PC3 cells were cultured in 10% CSS-RPMI medium with or without DHT (1 ng/mL) for 24 hrs. Invasion assays were performed and exogenous HGF was used to activate HGF/c-MET signaling. Anti-HGF neutralizing antibody was used to block HGF function. Cells (100000 cells per well for LNCaP, 20000 per well for PC3) were added and incubated in for 48 hrs and calcein AM (4 uM) were used to stain live cells. LNCaP cells (AR+/MET-) responded to HGF with increased invasiveness in the absence of DHT, and this impact was no longer observed in the setting of anti-HGF neutralizing antibody. In contrast, when AR signaling was maintained with DHT, so significant effect of HGF or anti-HGF was observed. In contrast, PC3 cells responded to HGF regardless of DHT administration, and anti-HGF had an inhibitory effect in both settings. Interestingly, anti-HGF resulted in lower than

baseline invasion levels for PC3 cells.

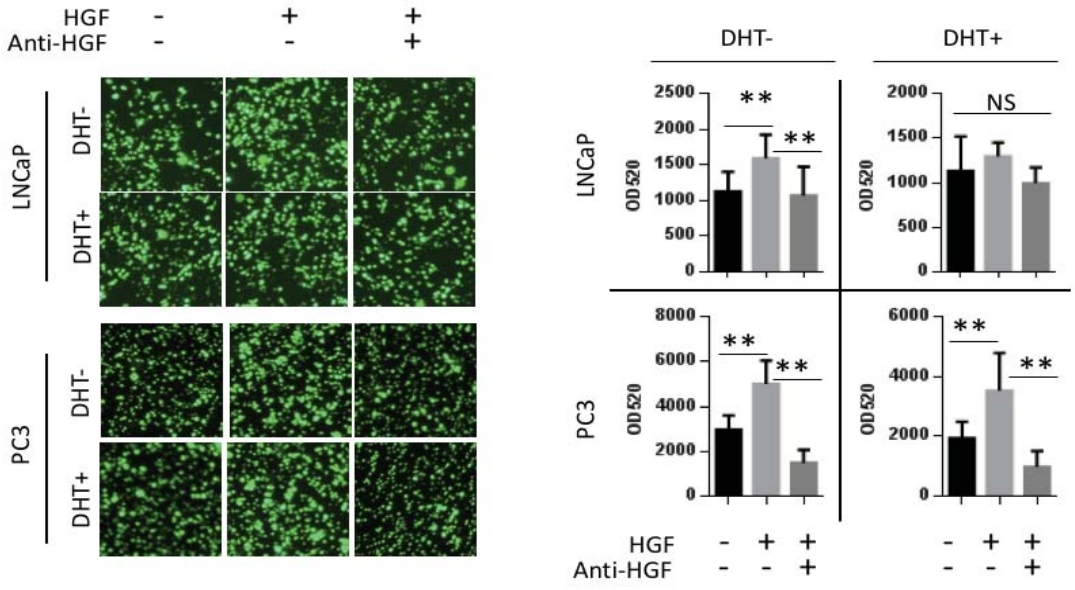

Figure 10: Invasion assays were performed in MET- (LNCaP) and MET+ (PC3) prostate cancer cell lines using DHT, HGF, and anti-HGF neutralizing antibody to elucidate the interaction between AR and MET for driving the invasive phenotype in these cell lines.

Subtask 4: *Assess whether c-MET siRNA, anti-HGF neutralizing antibody, and/or absence of HGF in the setting of enzalutamide administration recovers the effects of androgen suppression in vitro.*

We next sought to determine if MET expression results in a phenotype in AR+ CRPC models that is sensitive to MET inhibition. In light of the encouraging results for cabozantinib above, we continued to utilize cabozantinib for inhibition of the HGF/MET signaling pathway. As shown below, MET overexpression promoted invasion in AR^{+} LNCaP cells (in the presence of androgen), which was sensitive to cabozantinib. We then found that p-Met is increased upon HGF stimulation in MET-transfected LNCaP cells cultured in the presence of androgen and showed that exposure to cabozantinib reverses this effect. Importantly, cabozantinib had no effect on VCaP or LNCaP cell invasion under normal culture conditions (androgen present). However, when AR signaling in LNCaP cells was inhibited through the use of charcoal stripped medium, HGF significantly increased invasion in a cabozantinib sensitive manner.

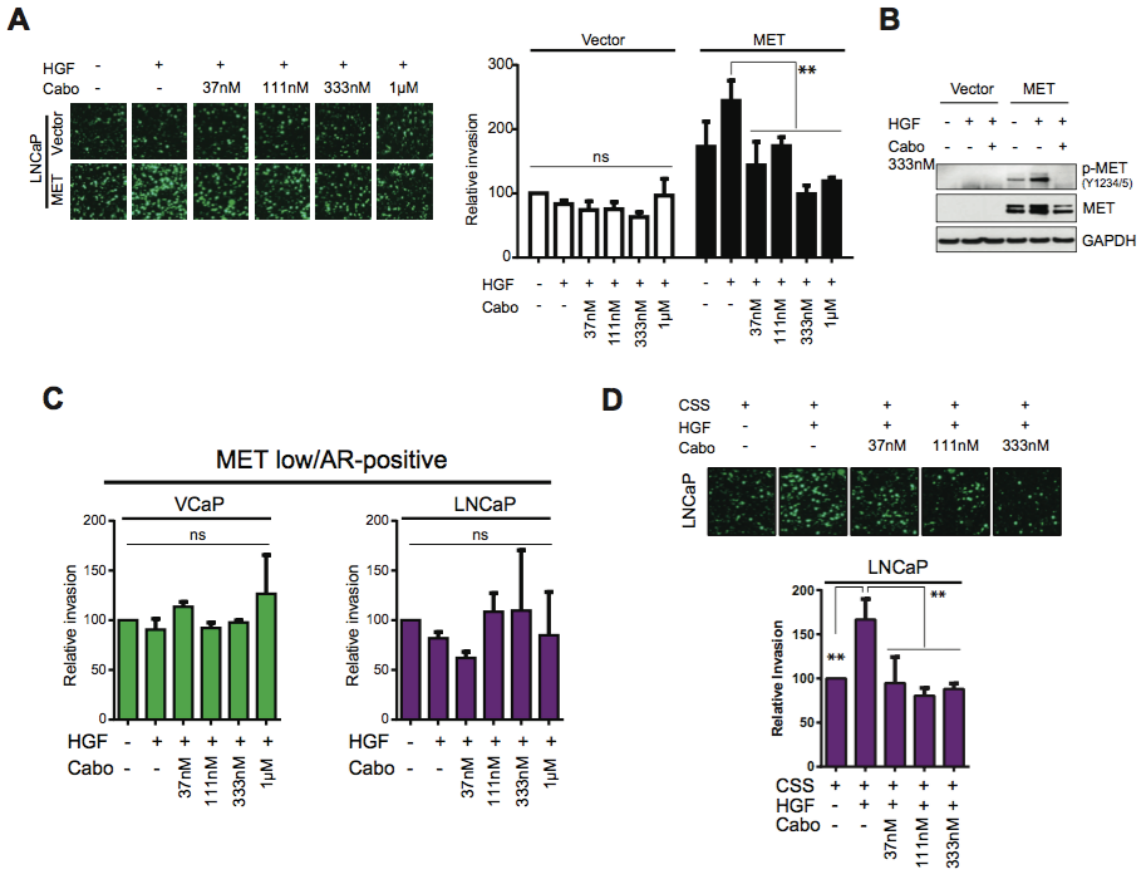

Figure 11: Elevated MET sensitizes AR$^+$ prostate cancer to cabozantinib. (**A**) LNCaP (AR$^+$) prostate cancer cells were stably transfected with either empty vector or MET, and invasion ability was assessed in the presence of HGF and/or various treatment doses of multityrosine kinase inhibitor cabozantinib (Cabo) as indicated. Left panel is representative pictures of indicated treatment results by fluorescent staining. Right panel is the quantification of invasion relative to vector control. (**B**) Selected treatment outcomes were measured by western blot for phospho-MET and total MET protein levels. (**C**) Invasion assays were performed in the presence of HGF and/or various treatment doses of cabozantinib (Cabo) in MET low/AR-positive prostate cancer cells for 48 hours. (**D**) LNCaP (AR$^+$) prostate cancer cells were treated with charcoal stripped serum (CSS) for 48 hours prior to invasion assay under indicated conditions for another 48 hours.

We then sought to better understand the impact of HGF and anti-HGF neutralizing antibody on c-MET expression and AR signaling. VCaP cells were cultured with with 10% DMEM media for 24 hrs. DHT (1 ng/mL) was then added with or without MDV3100 (10 μM) for another 24 hrs, and conditoned media from HS5 bone marrow stromal cells were then used to treat samples in the presence or absence of anti-HGF neutralized antibody (100 ng/mL). Expression of phosphor-ERK and c-MET were evaluated. As shown in the figure, p-ERK and c-MET expression increase with enzalutamide, which also suppresses PSA expression. In the presence of anti-HGF neutralizing antibody, c-MET and p-ERK expression are substantially suppressed with persistent suppression of PSA expression.

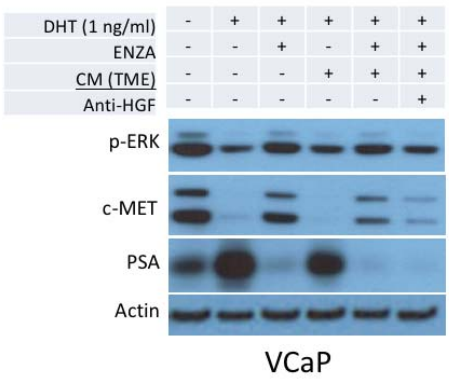

Figure 12: Exposure of VCaP cells to DHT, enzalutamide, conditioned media from HS5 cells, and anti-HGF neutralizing antibody to assess relationship of HGF/MET pathway and AR signaling activity in response to suppression of these pathways.

In order to further assess the interplay between enzalutamide and HGF, we cultured LNCaP cells with 10% CSS-RPMI plus DHT 1 ng/mL for 24 hrs and then treated with or without MDV-1000 (10 ug/mL) for 24 hrs. Invasion assays were performed with and without conditioned medium (CM) from the human bone marrow stromal cell line HS-5 and with and without enzalutamide. Additionally, anti-HGF neutralizing antibody was used to block HGF in the conditioned medium. Increased cell invasion was observed with CM, as expected, regardless of enzalutamide exposure. However, ant-HGF neutralizing antibody was only effective in the setting of enzalutamide administration, further confirming the central role of the HGF/MET axis in the setting of potent AR signaling inhibition.

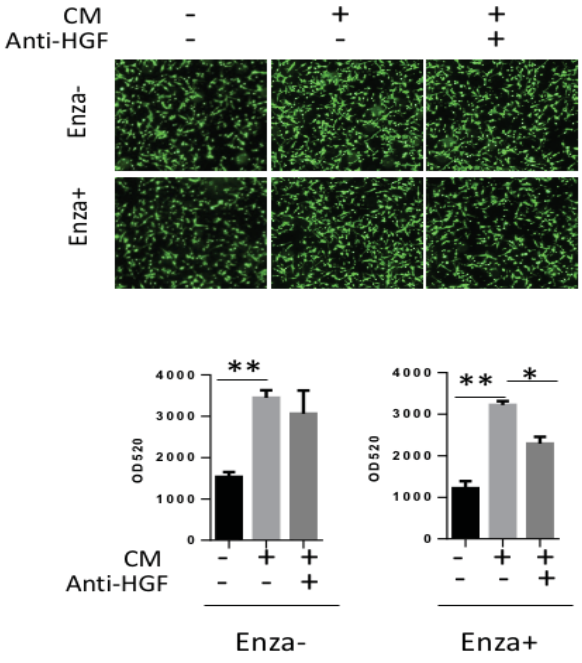

Figure 13: Invasion assays were performed using LNCaP cells. Conditioned medium (CM) from the human bone marrow stromal cell line HS-5 increases increases cell invasion both in the presence and absence of enzalutamide. Anti-HGF neutralizing antibody inhibits the effect of CM only in the setting of enzalutamide, supporting the role of the HGF/MET axis as a mechanism of resistance to enzalutamide.

Subtask 5: *Determine the interplay between cancer cell c-MET activity and the bone marrow microenvironment for facilitating resistance to enzalutamide using bone marrow stromal cells*

In order to further evaluate the role of the microenvironment in potentially facilitating resistance to enzalutamide, we again used CM from HS-5 bone marrow stromal cells and evaluated MET pathway activity under varying conditions. PC-3 cells only expressed p-MET in the setting of HGF, and this was reversed by anti-HGF antibody. p-ERK was also much more strongly expressed in the setting of HGF, indicating downstream pathway activity. While p-MET is generally not detectable in LNCaP cells, we saw increased p-ERK and p_AKT when enzalutamide was added in the presence of CM, and this was inhibitied by anti-HGF antibody. These data suggest that BMSCs can promote MET pathway activity in MET- PCa cells in the setting of enzalutamide.

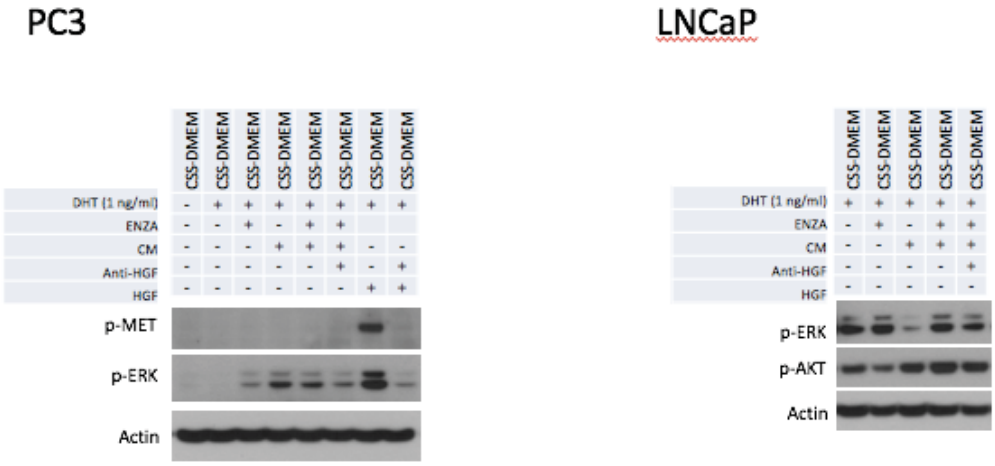

Figure 14: MET pathway activity was assessed via Western blot in PC-3 and LNCaP cells using CM from the human bone marrow stromal cell line HS-5 and in the presence/absence of enzalutamide, HGF, and anti-HGF antibody.

We hypothesized that macrophages discriminate between different types of apoptotic cells and orchestrate a distinctive response accordingly. To investigate the production of proinflammatory cytokines, co-cultures of macrophages and different highly apoptotic cells were analyzed. Two prostate cancer cell types (murine RM1 and human PC3) and 2 non-cancer cell types (murine osteoblastic MC4 and murine primary bone marrow stromal cells [BMSCs]) were used. Secreted proteins from co-cultures of macrophages and apoptotic cells were analyzed using inflammation arrays (Figure 15A), and results were quantified and normalized relative to macrophage-alone controls (Figure 15B). Cytokine activation of CCL5, CXCL1, CXCL5, IL-6, and IL-12 was observed in macrophages co-cultured with apoptotic cancer cells, but not apoptotic non-cancer cells.

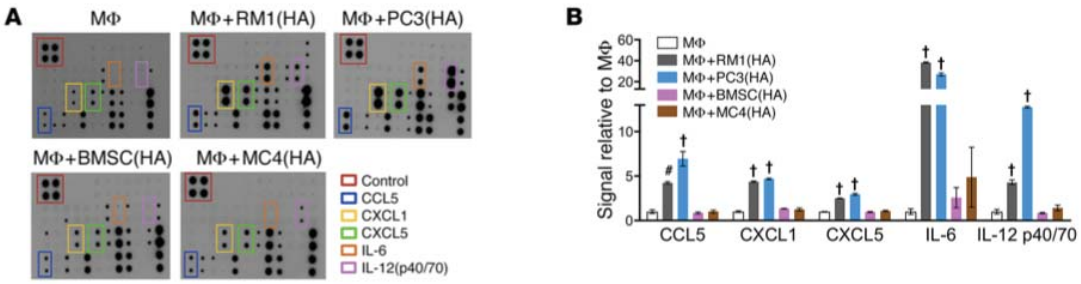

Figure 15: Inflammatory cytokine and transcription factor activation in co-cultures of macrophages and highly apoptotic (HA) cells. Supernatants were collected from macrophages (MΦs) alone or co-cultured with RM1(HA), PC3(HA), BMSC(HA), or MC4(HA) cells for 18–20 hours and analyzed via inflammatory cytokine array. (A) Representative images. (B) Quantification of cytokines induced.

ELISA evaluation for CXCL1 and CXCL5 proteins in the coculture media for apoptotic cancer cells (Figure 16) confirmed the cytokine array results and aligned with the mRNA analyses. Altogether, these results suggest that the clearance of apoptotic cells by macrophages induced a selective response dependent on the cell type engulfed and a common inflammatory expression pattern in macrophages efferocytosing apoptotic cancer cells.

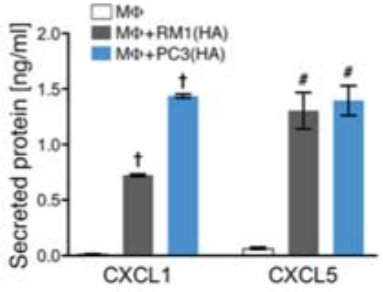

Figure 16: ELISA for total CXCL1 and CXCL5 levels in supernatants of MΦs alone or cocultured with RM1(HA) or PC3(HA).

We hypothesized that phagocytic monocytes/macrophages would increase serum levels of the inflammatory CXCL5 cytokine in bone metastasis patients because of tumor cell clearance both in circulation and in the bone marrow compartment. A cohort of serum samples from patients with progressive advanced castration-resistant prostate cancer metastatic to bone with multiple lesions (≥3 lesions), with no prior chemotherapy for metastatic disease and no signs of ongoing infection or another malignant disease, was analyzed. These samples were compared with cohorts of patients with either localized high-risk prostate cancer or non- cancer patients. All samples were analyzed by ELISA to measure 3 closely related cytokines: CXCL5, CXCL6 (a human cytokine homologous to mouse CXCL5), and IL-8 (CXCL8). Intriguingly, normal samples displayed significantly higher serum CXCL5 relative to localized cancer samples (Figure 17A). Importantly, considerably higher levels of CXCL5 were detected in the serum of bone metastatic patients compared with other groups, while no significant differences were observed for CXCL6 (Figure 17B). Contrary to the CXCL5 results, serum samples from bone-metastatic patients showed significantly reduced IL-8 concentrations relative to normal and localized samples (Figure 17C). Furthermore, no significant correlation was found between the CXCL5 or IL-8 serum concentrations and the age of patients for each group, respectively.

Altogether these findings suggest an important role for proinflammatory CXCL5 in prostate cancer bone metastasis and in facilitating resistance to androgen signaling inhibitor therapy.

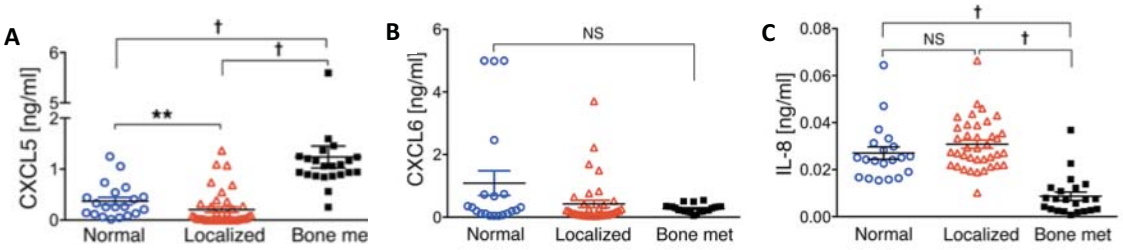

Figure 17: Human serum isolated from normal (n = 20), localized (high-risk) prostate cancer (Localized, n = 40), and bone-metastatic prostate cancer (Bone met., n = 22) patients was analyzed by ELISA for CXCL5 (A), CXCL6 (B), and IL-8 (C). CXCL6 and IL-8 analysis included n = 38 for Localized. Data are mean ± SEM; **P < 0.01, ***P < 0.001, ****P < 0.0001 (Wilcoxon 2-sample test and Kruskal-Wallis test with Bonferroni's correction).

Major Task 2: *Isolation and characterization of CTCs and DTCs in patients with mCRPC on conventional ADT or enzalutamide*

There have been 3 publications to date related to Major Tasks 2 and 3. One additional article is currently in revision at Neoplasia.

Singhal, U, Wang, Y, Henderson, J, Niknafs, Y, Gursky, A, Zaslavsky, A, Smith, DC, Chang, L, Feng, FY, Palapatu, GS, Taichman, RS, Chinnaiyan, A, Tomlins, S, **Morgan, TM**: Multigene profiling of a circulating tumor cells in mCRPC identifies clinically relevant prognostic signature, Multigene profiling of CTCs in mCRPC identifies a clinically relevant prognostic signature. Mol Cancer Res 16(4): 643-654, 2018. PM29453313

Hovelson DH, Liu CJ, Wang Y, Kang Q, Henderson J, Gursky A, Brockman S, Ramnath N, Krauss JC, Talpaz M, Kandarpa M, Chugh R, Tuck M, Herman K, Grasso CS, Quist MJ, Feng FY, Haakenson C, Langmore J, Kamberov E, Tesmer T, Husain H, Lonigro RJ, Robinson D, Smith DC, Alva AS, Hussain MH, Chinnaiyan AM, Tewari M, Mills RE, **Morgan TM***, Tomlins SA* (*co-senior authors): Rapid, ultra low coverage copy number profiling of cell-free DNA as a precision oncology screening strategy. Oncotarget 8(52): 89848- 89866, 2017. PM29163793/PMC5685714

Kozminsky, M, Fouladdel, S, Chung, J-S, Wang, Y, Smith, D.C., Alva, A, Azizi, E, **Morgan, T.M.***, Nagrath, S.* (*co-senior authors), Detection of CTC Clusters and a Dedifferentiated RNA-Expression Survival Signature in Prostate, Advanced Science 6(2): 1801254, 2018. PMC6343066

Subtask 1: *Human subjects protocols already submitted and approved for all aims*

This was completed at the beginning of the funding period

Subtask 2: *Blood obtained from 20 patients with mCRPC progressing on conventional ADT and 15 patients progressing on enzalutamide. Bone marrow obtained from subset of these patients.*

During the funding period, we were able to obtain blood from a total of 18 patients with mCRPC progressing on conventional ADT and 16 patients progressing on enzalutamide. Bone marrow obtained from 4 of these patients.

Subtask 3: Detection and isolation of CTCs/DTCs from blood and BM aspirates

During the initial period of the grant, due to difficulty recruiting patients for BM aspiration, we focused on refining our approach to CTC isolation and determining expression of key prostate cancer genes in these patient samples Over time, we were able to consistently measure gene expression in CTCs and DTCs across a panel of 96 genes. For platform validation, 180 GFP labeled prostate cancer cells (PC3, LNCaP, VCaP) were sorted into 5 mL whole blood from a normal donor. Cells were captured using an immunomagnetic bead enrichment and visualized by immunofluorescence. Cells were then counted to assess for recovery rate. Additionally, 300 PC3 & LNCaP cells were spiked into 5 mL of whole blood from healthy controls and captured by immunomagnetic bead enrichment, followed by staining with DAPI, CD45, and PCa-CT (antibody cocktail, PSMA, EGFR, and pan-cytokeratin). To validate gene expression after CTC isolation, 10 prostate cancer cells (PC3, LNCaP, VCaP) were spiked into 5 mL whole blood from a normal control. Gene expression was then expressed by qPCR to assess whether the expression pattern matched that of what was expected for PC3, LNCaP, and VCaP cells.

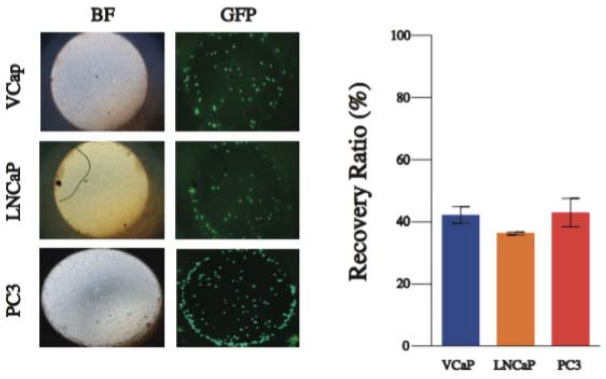

Figure 18: GFP-labeled LNCaP, VCaP, and PC3 cells were spiked into whole blood and retrieved using immunomagnetic bead enrichment.

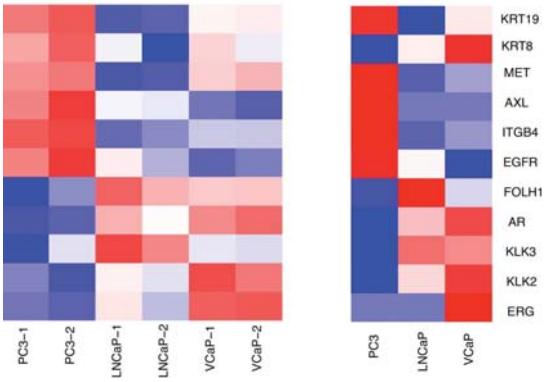

Figure 19: 10 cells at a time from each cell line were spiked into 5mL of whole blood. Gene expression was measured after immunomagnetic bead selection (left panel) and compared with known baseline gene expression data (right panel) from each of these lines.

Finally, for DTC processing, over the past several years, we have refined our approach using 2 distinct methodologies. These are described in more detail below.

a) *Anti-EPCAM bead enrichment, mRNA isolation, and qRT-PCR*: Isolation of DTCs from 1 ml of bone marrow aspirate was performed as described for peripheral blood[26]. Briefly, cells were bound to anti-EPCAM magnetic beads, washed, and directly lysed. mRNA was captured with Oligo(dT) 25 mRNA Dynabeads (Thermo Fisher Scientific) and reverse transcribed into cDNA. No cell enumeration is conducted with this approach. Preamplification of up to 96 genes including controls was performed followed by qRT-PCR and relative quantification by the ΔΔCt method. To assess the validity of this approach, we have compared metastatic samples, localized prostate cancer patient samples, and healthy controls. We found that metastatic patients cluster with the "PCa positive 2" population, but that DTCs are also detectable in patients with localized prostate cancer.

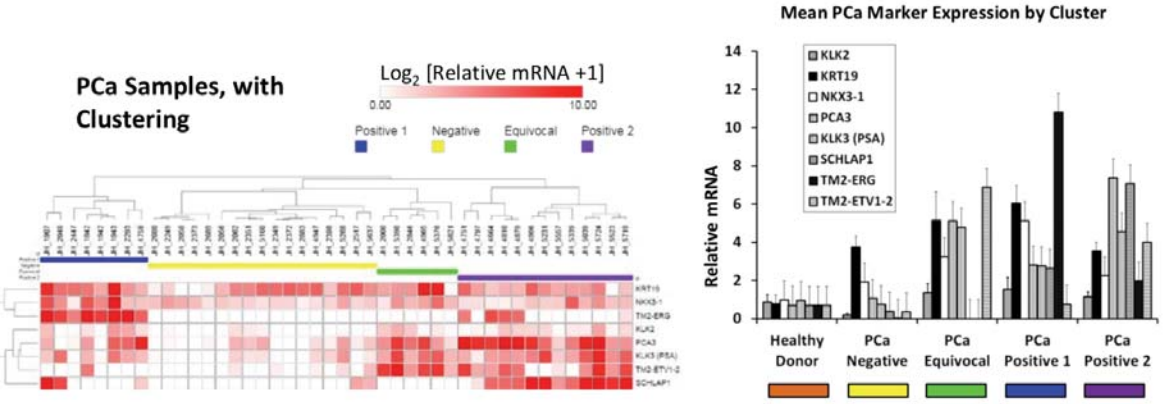

Figure 22: Left- Hierarchical clustering of marker gene expression in the PCa patients. Of the three main clusters, the outside two clusters are hypothesized to contain DTCs ("Positive 1" (blue) and "Positive 2"(purple)). The middle cluster is hypothesized to be "Negative" (yellow) or "Equivocal" (green) for the presence of DTCs. Right- Mean ± SEM expression of the marker genes grouped by healthy donor or the four PCa patient expression clusters.

DTC enrichment and/or isolation by FACS: Marrow aspirates were mixed 1:1 with PBS, layered onto Ficoll (GE Healthcare #17-1440-02) and centrifuged at 500 x G for 30 minutes to isolate the buffy coat / nucleated population. Subsequent steps were performed in cold flow cytometry buffer (PBS with 2% FCS and 1 mM EDTA). We initially sorted cells negative for CD45 and positive for any level of surface EPCAM expression as putative DTCs – termed "Lenient" approach. We then added negative markers for erythroids (CD235a), hematopoietic stem and progenitor cells (CD34), osteoblastic lineage cells (alkaline phosphatase) and increased the threshold for EPCAM positivity five-fold – termed the "Stringent" approach (Figure). We set a threshold of greater than 5 cells per million single, viable buffy coat cells. This threshold was selected at a local minimum of a histogram of the frequency of these cells in patients with localized PCa (Figure). Using this threshold of > 5 per million cells, we detected the presence of the putative DTC population in 3 of 6 metastatic PCa patients. With regard to the one normal donor with this population present, we also note that these methods could theoretically detect any epithelial cancer and at present we are unable to exclude this possibility. Certainly, this could also be indicative of a false positive result.

Marker	Target
DAPI	Viable cells
CD45	Leukocytes
CD235a	Erythroid cells
alkaline phosphatase	Osteoblastic lineage
CD34	HSCs and progenitors
EPCAM / CD236	Epithelial cells

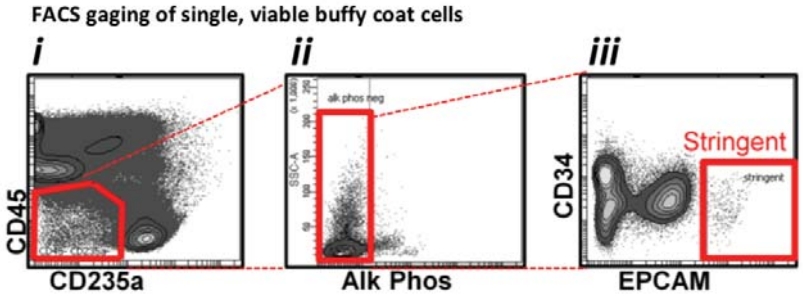

Figure 23: Analysis and Isolation of putative DTCs using multi-parameter FACS; "Stringent" approach using three additional markers and higher EPCAM threshold. Flow cytometry markers and gating strategy are shown.

Subtask 4: *Molecular characterization of AR and HGF/c-MET axis in isolated CTCs/DTCs. Approaches used for characterization will include qRT-PCR, IHC, and flow cytometry.*

To characterize the CTC gene expression pattern in patients, we evaluated 41 patients with mCRPC. The median age was 68 (IQR 61–75) and median PSA was 19.7 ng/mL (IQR 3.6–70.6 ng/mL). At the time of enrollment, all patients were on luteinizing hormone releasing hormone (LHRH) agonist therapy (leuprolide and goserelin), 5 patients were on additional treatment with abiraterone, 11 on enzalutamide, 8 on docetaxel, 4 on cabazitaxel, 1 on radium 223, and 1 on dexamethasone. Patients had received a median of two prior therapies (IQR 1–3). All patients had a minimum of 90 days follow-up and there were 21 (51.2%) deaths. The median time to next therapy was 251 days (IQR 119–329) and patients received a median of one subsequent therapy (IQR 0–1). 27 patients were CTC-positive. Of these, 19 samples (70%) showed increased expression of AR and 15 (55%) showed significant expression of AR-V7, with 14 (52%) shared between these two groups. Increased down- stream AR signaling was seen in 14 (52%) samples based conjoint expression of KLK2 (PSA) and NKX3-1, and 18 (67%) samples showed significant upregulation of Wnt signaling based on expression of WNT5a, WNT5b, and BMP7. Among epithelial–mesenchymal transition (EMT) genes, 9 samples (33%) expressed SOX2 and 21 (67%) had elevated levels of TWIST1, with 7 samples (26%) expressing both genes. Similarly, clustering jointly on MDK and CCNA2, 15 samples (56%) showed high levels of cell cycle activity. Among long noncoding RNAs (lncRNA) associated with prostate cancer, 19 samples (70%) showed elevated levels of the lncRNA SChLAP1, but only 8 (30%) showed increased PCA3 levels. The TMPRSS2:ERG gene fusion was significantly expressed in 11 samples (41%) and based on concordant expression across two distinct amplicons, evidence for the TM2:ETV1 fusion was seen in 4 samples (15%; Figure 24).

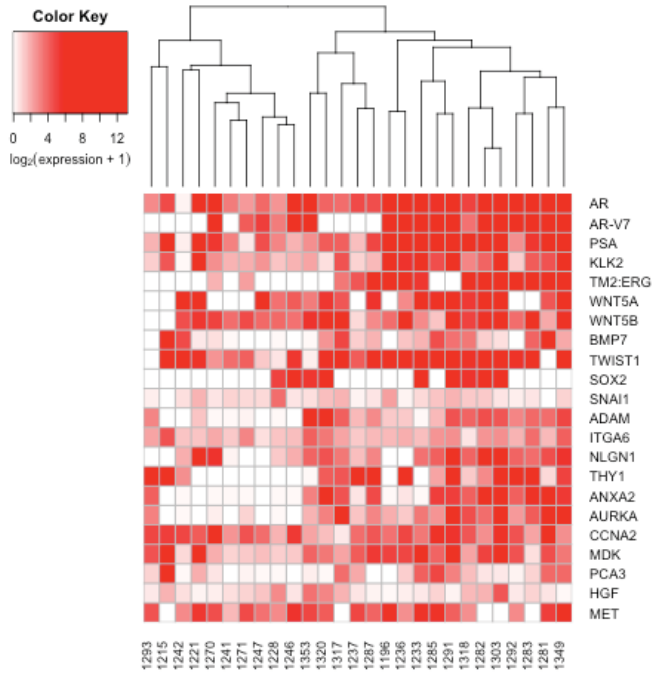

Figure 24: Heatmap illustrating gene expression of prostate cancer-related genes determined from CTCs in mCRPC patients. Expression was normalized to internal housekeeping genes for each patient and to average expression in a set of normal controls in order to control for background contamination from lymphocytes.

Based on our initial analyses, CTC-based expression of AURKA (HR 3.40, 95% CI 1.47 – 7.85), WNT5a (HR 2.71, 95% CI 1.43 – 5.13), and BMP7 (HR 2.1, 95% CI 1.25 – 3.52) all appear to be strong predictors of mortality in this patient population.

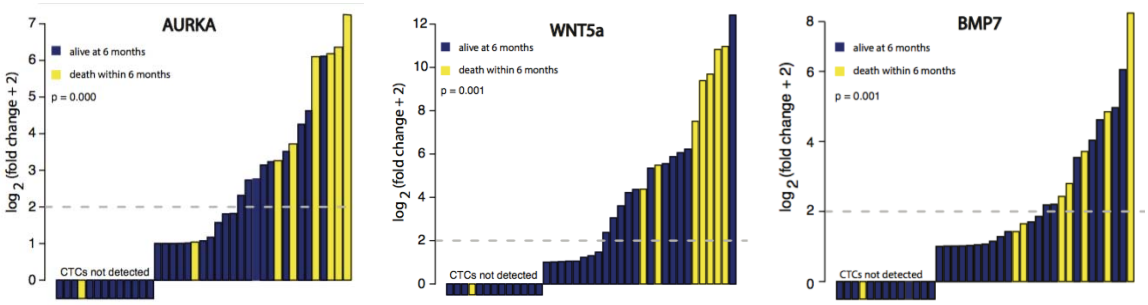

Figure 24: Waterfall plots showing association between expression of AURKA, WNT5a, and BMP7 in CTCs with early mortality among a cohort of patients with advanced mCRPC.

In addition, we have used ELISA to assess HGF expression in the plasma of patients progressing on enzalutamide treatment. Duplicates were used for each sample, and serially diluted HGF was used to generate a standard curve for comparison. We found marked increase in HGF expression in patients progressing on enzalutamide compared to normal controls, in line with our hypothesis that HGF expression may be driven up in the setting of enzalutamide resistance.

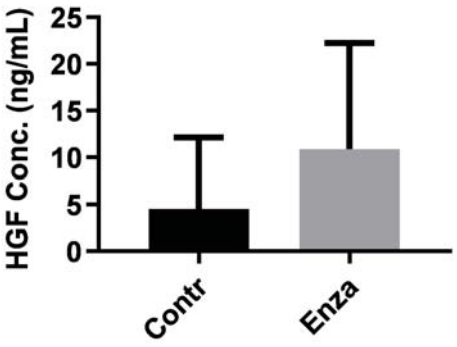

Figure 25: ELISA was used to measure HGF expression in the plasma of control samples compared to those progressing on enzalutamide.

To increase statistical power in our initial analyses, we have combined the enzaltamide and abiraterone cohort, and gene expression results are shown below.

Compared to patients who were CTC-negative or ARSI responders, patients who were CTC-positive or ARSI non-responders tended to express genes that are related to prostate cancer or AR signaling (Fig. 26).

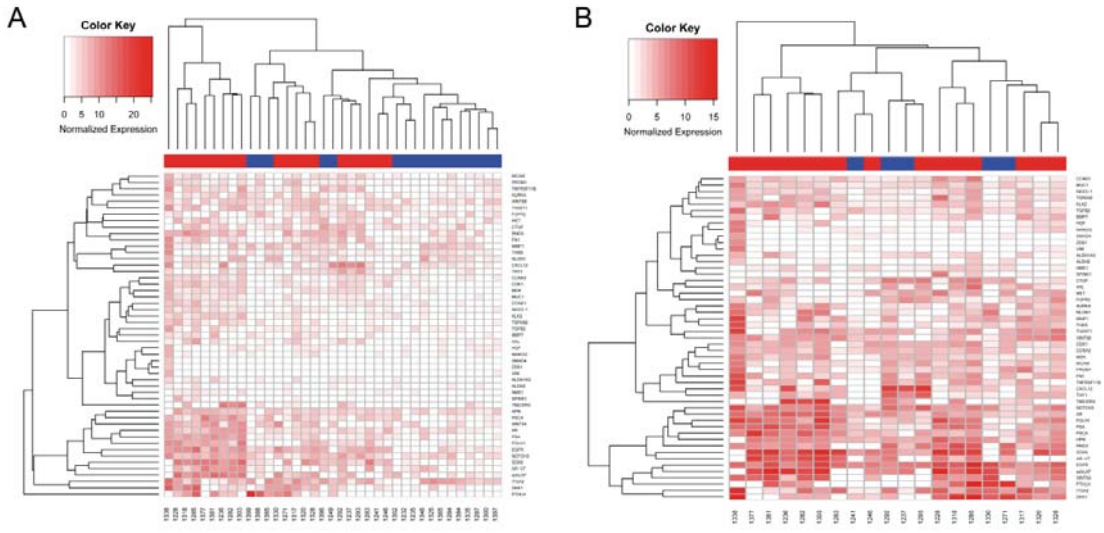

Figure 26: Integrative gene expression analysis. (A) Heat map comparing gene expression data from CTC-positive samples (red) and CTC-negative samples (blue). (B) Hierarchical clustering of gene expression in CTC-positive patients only. The 51 selected genes were enriched in patients with a PSA response (blue), compared to patients without a PSA response (red).

Subtask 5: *Analysis to determine c-MET pathway activity in enzalutamide vs. non-enzalutamide treated patients and potential role of HGF/c-MET pathway in supporting resistance to enzalutamide*

At the time of the present analyses, we did not find any correlation between HGF/c-MET expression and resistance to enzalutamide in this cohort. However, additional follow-up data will yield a greater number of events, and we will be able to assess this correlation again with further follow up.

Major Task 3: *Assess interplay between tumor HGF/c-MET pathway activity and response to abiraterone, and identify potential mechanisms of abiraterone resistance*

Subtask 1: *Blood obtained from 25 patients with mCRPC initiating abiraterone. Bone marrow obtained from a subset of these (goal of 3).*

We have obtained blood from a total of 20 patients with mCRPC initiating abiraterone. Bone marrow obtained from 3 of these patients.

Subtask 2: *Detection and isolation of CTCs/DTCs from blood and BM aspirates, and bone marrow HGF expression measured by ELISA*

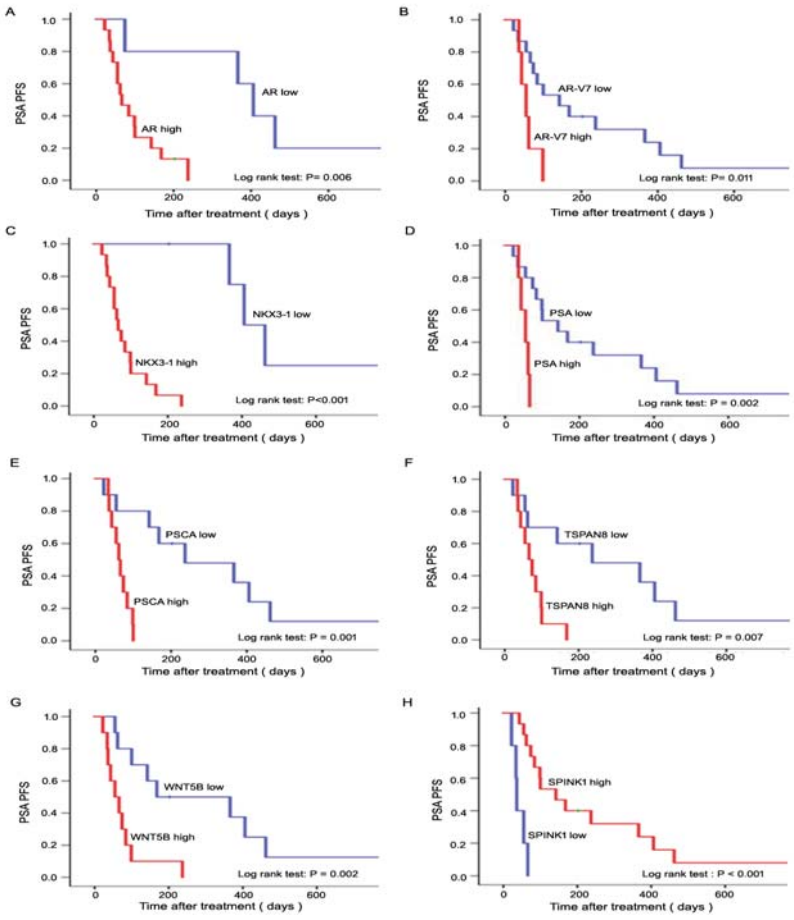

CTCs/DTCs were isolated as described above in Major Task 2/Subtask 2. CTC characterization led to identification of a number of genes associated with response to androgen receptor signaling inhibition (here, enzalutamide and abiraterone are analyzed together to increase statistical power – additional follow-up will be necessary to assess these separately). Key genes are shown in the figure at left.

Figure 27. PSA PFS as a function of gene expressions (A: AR, B: AR-V7, C: NKX3.1, D: PSA, E: PSCA, F: TSPAN8, G: WNT5B, H: SPINK1). P value from log rank test.

Subtask 3: *Molecular characterization of AR and HGF/c-MET axis in isolated CTCs/DTCs using qRT-PCR, IHC, and flow cytometry as well as targeted sequencing*

To identify markers of treatment response and resistance in CTCs, we evaluated 89 prostate cancer-related genes and 3 internal controls from isolated CTCs. Using our epithelial-based expression signature to assess for the presence of CTCs, twenty patients (54%) were classified has having evaluable CTCs. Gene screening was performed using a clustering algorithm, and based on this analysis, 41 genes (30 prostate cancer-related genes as well as the 8 epithelial markers and 3 internal control) were excluded, and 51 genes were retained for the survival analysis.

The number of patients in the high expression category varied for each of these genes: AR (75%), AR-V7 (25%), PSA(25%), PSCA(50%), SPINK1(75%), TSPAN8(50%), NKX3-1(75%), and WNT5B(50%). Univariable Cox regression analyses also supported the association with both PSA and radioclinical PFS for each of these genes. Additionally, BMP7, CCND1, FOLH1, SOX9, and WNT5a were significantly associated with PSA PFS, while THY1, PTHLH, MDK, and HGF were associated with radioclinical PFS. Waterfall plots displaying the maximum PSA response among CTC positive patients and correlation with each of the candidate genes are shown in Figure 28.

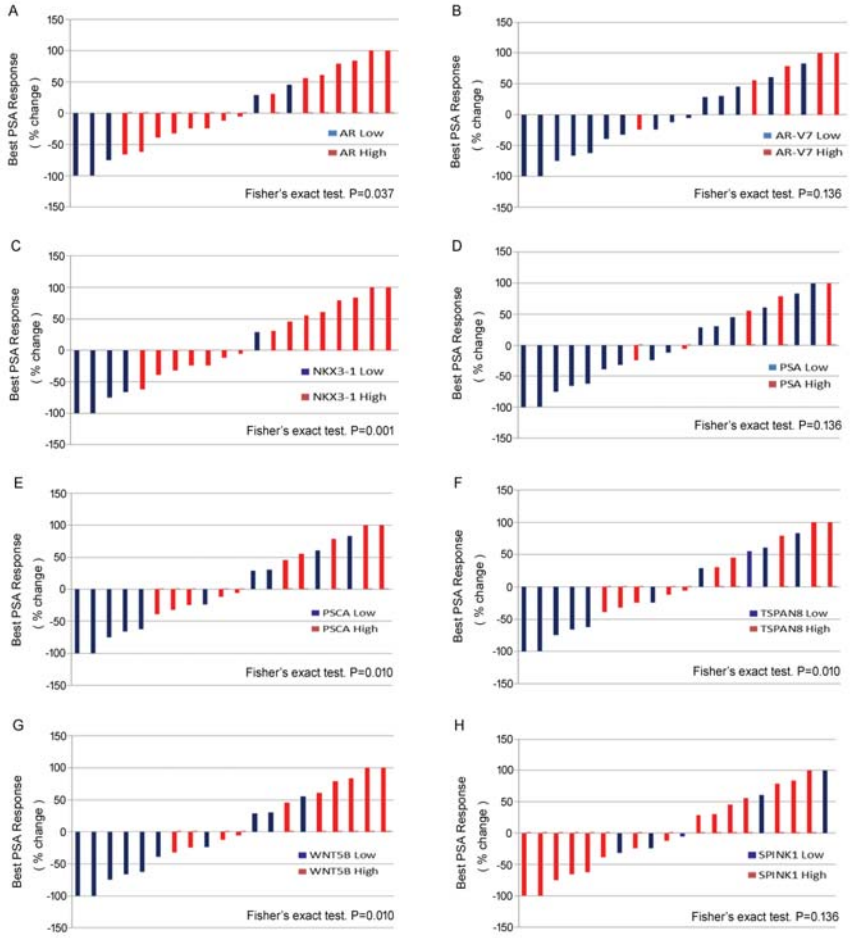

Figure 28. Waterfall plots displaying the PSA response to androgen receptor signaling inhibitors according to eight gene expressions. The best PSA response – 50% change line indicates the threshold for defining a PSA response (≥50% decline in PSA level from baseline). (A: AR, B: AR-V7, C: NKX3.1, D: PSA, E: PSCA, F: TSPAN8, G: WNT5B, H: SPINK1).

The overall proportion of patients with a PSA response (≥50% decline from baseline) was 25% (5/20), and non-response to ARSI treatment was significantly associated with high expression of AR, TSPAN8, PSCA, WNT5B, and NKX3-1. Finally, AR, AR-V7, WNT5B, and SPINK1 were all associated with overall survival in the Kaplan-Meier analyses for this secondary endpoint.

In addition, over the past year we have performed whole genome amplification and whole exome sequencing to ~100x coverage of leukocytes and putative DTCs from 5 localized PCa patients, one metastatic patient, and the PC3 cell line. The leukocyte population was used as an internal control for each patient. The sample from one of the localized PCa patients was sent for sequencing directly after isolation (yellow), whereas the other four samples utilized material previously used for qRT-PCR (orange). To determine if these populations contained small alterations characteristic of PCa, we based our analysis on a list of 75 genes previously reported to be altered in PCa. **Figure 29A** reports genes from this list which had either single nucleotide polymorphisms (SNPs) or gene level structural variants (SVs) in the putative DTC population but not in the corresponding leukocyte control, to guard against detection of germline alterations or technical artifacts. In addition to the metastatic sample and the control cell line, we observed alterations of PCa genes in two of the 5 localized PCa samples. Unfortunately, the data was not of sufficient quality to visualize chromosomal level alterations (deletions, amplifications, and translocations), likely due to unequal amplification across the genome, which has been reported previously with the Repli-G whole genome amplification system. Lastly, to gain an appreciation for the approximate fraction of cancer cells in the putative DTC population, we examined the allele frequency for SNPs. The allele frequency was higher for the metastatic sample compared to the localized PCa samples (**Figure 29**).

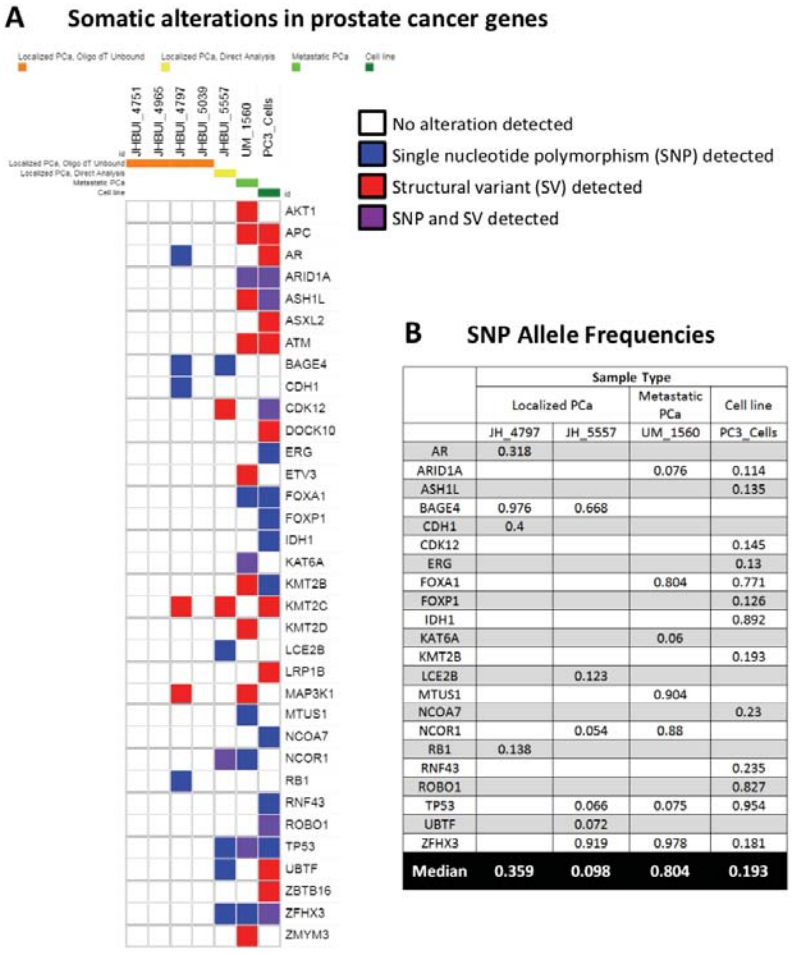

B **SNP Allele Frequencies**

	Sample Type			
	Localized PCa		Metastatic PCa	Cell line
	JH_4797	JH_5557	UM_1560	PC3_Cells
AR	0.318			
ARID1A			0.076	0.114
ASH1L				0.135
BAGE4	0.976	0.668		
CDH1	0.4			
CDK12				0.145
ERG				0.13
FOXA1			0.804	0.771
FOXP1				0.126
IDH1				0.892
KAT6A			0.06	
KMT2B				0.193
LCE2B		0.123		
MTUS1			0.904	
NCOA7				0.23
NCOR1		0.054	0.88	
RB1	0.138			
RNF43				0.235
ROBO1				0.827
TP53		0.066	0.075	0.954
UBTF		0.072		
ZFHX3		0.919	0.978	0.181
Median	**0.359**	**0.098**	**0.804**	**0.193**

Figure 29: Whole genome amplification and whole exome sequencing of the putative DTC population. **A,** Map showing somatic single nucleotide polymorphisms (SNPs) or small structural variants (SVs) detected in each experimental sample but not $CD45^+$ cells from the same patient as a germline control. Sample types are annotated as follows: orange; localized PCa patient samples with material sent for sequencing after mRNA purification, yellow; localized PCa sample processed for sequencing directly, light green; metastatic PCa sample used as

positive control for FACS, dark green; PC3 cell line used as a positive control for sequencing. Detected alterations are indicated by: white; no alteration detected, blue; SNP detected, red; SV detected, purple; SNP and SV both detected. **B,** Allele frequencies for SNPs from the two localized PCa samples with detected alterations, the metastatic sample, and PC3 cells. The median allele frequency for each sample is listed in the bottom row.

Subtask 4: *Blood obtained from 25 patients with mCRPC progressing on abiraterone (matched serial samples with Subtask 1 patients where possible, estimate 10 patients matched). Bone marrow obtained from subset of these patients (goal of 3).*

We obtained blood from a total of 19 patients with mCRPC progressing on abiraterone. Bone marrow obtained from 2 of these patients.

Subtask 5: *Bone marrow HGF expression measured, and CTCs/DTCs isolated and similarly characterized as in Subtask 3.*

Due to the paucity of bone marrow samples, we focused this analysis on plasma HGF. Here, we performed ELISA to compare plasma HGF expression in patients progressing on abiraterone compared to those progressing on standard ADT or enzalutamide. Interestingly, unlike enzalutamide, patients on abiraterone did not have any significant increase in plasma HGF compared to controls.

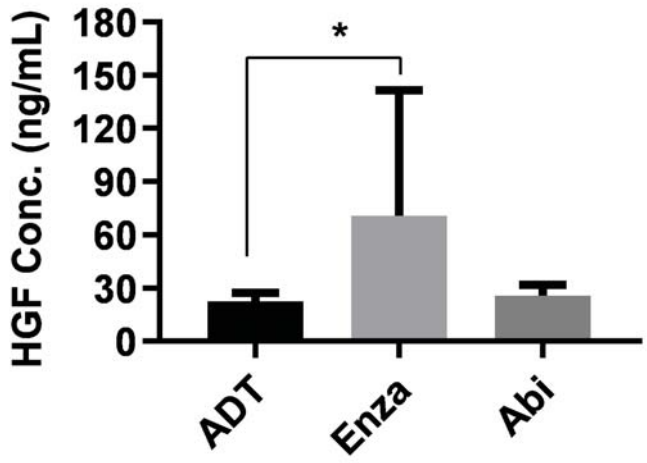

Figure 30: ELISA was used to measure HGF expression in the plasma of patients progressing on abiraterone compared to those progressing on enzalutamide or standard ADT.

Subtask 6: *Patients followed clinically for progression on abiraterone.*

All surviving patients have continued to undergo regular follow-up.

Subtask 7: *Changes in HGF/c-MET pathway expression identified prior to initiation of abiraterone and at 6 months will be correlated with patient response*

Based on our analyses to date, we have not identified a correlation between changes in HGF/MET expression over time and patient response to abiraterone. We will reassess this question after additional patient follow-up.

Subtask 8: *Additional pathways associated with PCa progression and cancer stem cell characteristics will be evaluated to identify other potential mechanisms of resistance to abiraterone*

To attain sufficient statistical power beyond exploratory analyses, we combined the enzalutamide and abiraterone datasets for identification of mechanisms of resistance to androgen signaling inhibition. Among CTC-positive patients, the median times to PSA progression and radioclinical progression were 91 days (IQR: 55–228 days) and 142 days (IQR: 42–492 days), respectively. Among the 51 candidate genes, increased expression of AR, AR-V7, PSA, PSCA, TSPAN8, NKX3-1, and WNT5B were significantly associated with decreased PSA PFS and radioclinical PFS, while SPINK1 was inversely associated with these outcomes. Univariate Cox regression also supported the association with both PSA and radioclinical PFS for each of these genes (Fig. 31). Of note HGF ranked near the top for both endpoints. Additionally, BMP7, FOLH1, SOX9, and WNT5a were nominally associated with PSA PFS, while THY1, PTHLH, and MDK were associated with radioclinical PFS

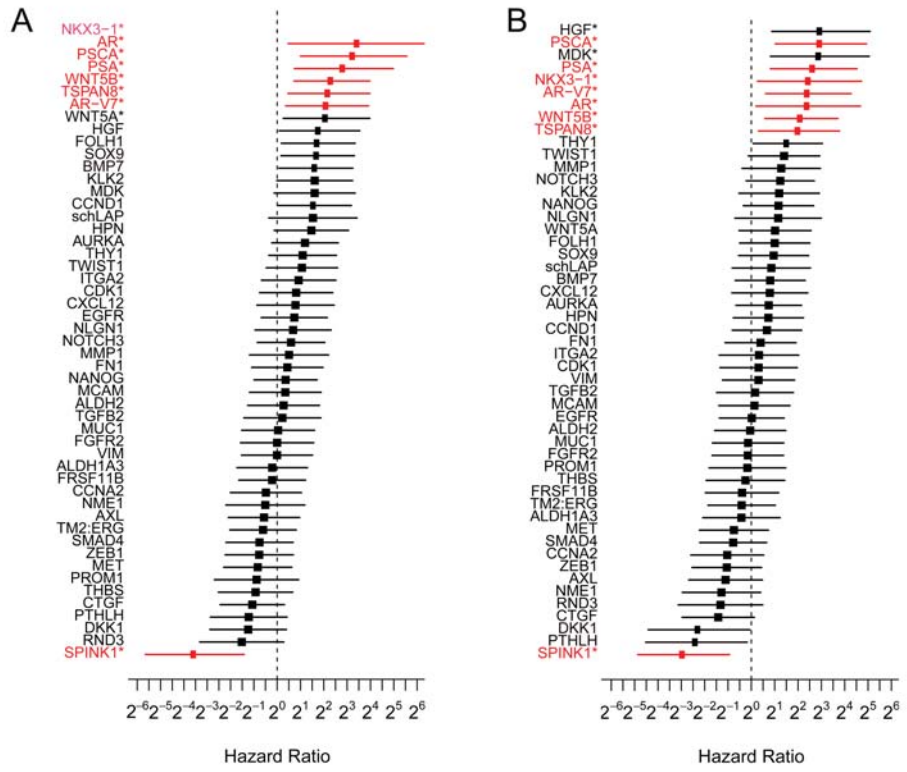

Figure 31. Gene signatures that can predict the response to androgen receptor signaling inhibitors. Cox proportional hazard analyses of the associations between individual gene signatures and prostate-specific antigen progression-free survival (PSA PFS) (A) or radioclinical PFS (B). Gene names shown in red were statistically significant for both clinical outcomes.

Subtask 9: *Data compilation/organization and statistical analysis to determine molecular characteristics associated with abiraterone response and with acquired resistance to abiraterone*

A multi-gene model comprised of all candidate genes (AR, AR-V7, PSA, PSCA, TSPAN8, WNT5B, NKX3-1, and SPINK1) was developed and compared to a single-gene model for AR-V7 (Fig. S5). Receiver operating curves were constructed, and the AUCs for the multi-gene model showed increased accuracy compared to AR-V7 alone for PSA PFS (0.84 vs. 0.65) and radioclinical PFS (0.86 vs. 0.64).

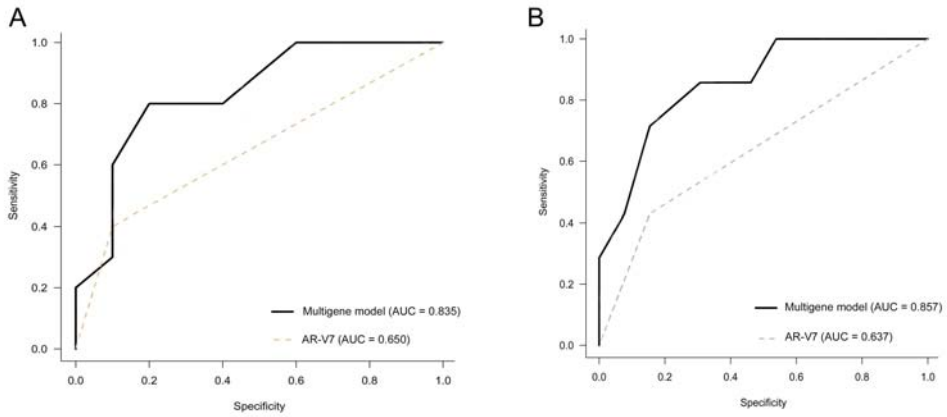

Figure 32: ROC curves for multigene models for PSA PFS (A) and radioclinical PFS (B)

Key Research Accomplishments

Research accomplishments:

- Publication of 7 manuscripts based on this work
- Two additional manuscripts based on Aims 2 and 3 in submission
- Identification of cytokine activation in macrophages exposed to apoptotic cancer cells.
- Demonstration that clearance of apoptotic cells by macrophages induces a selective response dependent on the cell type engulfed
- Nomination of secreted CXCL5, due to tumor cell clearance by macrophages, as a driver of bone metastasis and resistance to androgen signaling inhibitor therapy
- Initial assessment of CTCs in patients on abiraterone and enzalutamide demonstrates ability to measure tumor cell gene expression in this setting
- Identification of a number of genes beyond AR-V7 which carry prognostic implications in patients undergoing abiraterone or enzalutamide treatment: AR, PSA, PSCA, TSPAN8, NKX3-1, WNT5B, and SPINK1.
- Development of a novel rapid, high-throughput approach to cfDNA interrogation in mCRPC patients
- Development of two novel approaches to DTC identification and subsequent molecular interrogation
- Submitted R01 September 2018
- Co-leader of SPORE project submitted September 2018

Training accomplishments:

- Completion of R01 boot camp program at University of Michigan for training in grant writing
- Consensus member: Sidney Kimmel Cancer Center at Jefferson—The Role of Genetic Testing for Inherited Prostate Cancer Risk
- Attended and presented at multiple conferences, including ASCO, AUA annual meeting, Society of Urologic Oncology annual meeting, Prostate Cancer Foundation meeting, PCF Coffey-Holden meeting, and European Association for Urology annual meeting
- Continue as instructor/faculty of medical school/graduate courses

Conferences/journal clubs:

- Attend monthly prostate cancer seminars
- Meet with mentors (Drs. Taichman and Chinnaiyan) regularly to discuss research progress/career development
- Continue leadership/active roles in Urology Grand Rounds, GU tumor board, P01 collaborative conferences
- Participation in NCI Cancer Moonshot BloodPAC initiative
- Participated in multiple study sections, including Ontario Institute for Cancer Research and American Urological Association. Standing member of American Cancer Society Committee on Clinical Cancer Research and Epidemiology Study Section.
- Named Associate Editor for prostate cancer at European Urology

Clinical responsibilities

- Continue Urology clinic
- Continue operative schedule

Professional accomplishments: President of Young Urologic Association sub-committee of SUO, Assistant Editor at Urologic Oncology, Associate Editor of European Urology (Impact Factor 17), SUO Young Investigator Award (2018). Invited lectures at Cleveland Clinic, University of Virginia, and University of Cincinnati.

Impact

1) What was the impact on the development of the principal discipline(s) of the project?

We have made a number of key strides related to tumor cell dissemination by studying circulating tumor cells (CTCs), cell-free DNA (cfDNA), and disseminated tumor cells (DTCs) in metastatic prostate cancer. Our work on CTCs has led to the development of a multiplex gene expression prognostic assay for men with metastatic castration-resistant prostate cancer. We have also developed a novel approach to performing high-throughput assessment of cfDNA, published in Oncotarget. Our work on DTCs has been heavily cited and lends support to the concept of tumor cell dormancy, and we have developed and refined two new approaches to DTC isolation and characterization. We have now developed molecular signatures of resistance to androgen signaling inhibition in metastatic prostate cancer using a CTC-based assay, and this work is currently in the submission process. We believe these efforts will continue to yield advances in moving towards liquid biopsy approaches to guide treatment selection in this disease setting.

Separately, these efforts have also helped position the PI at the forefront of efforts to understand how heritable mutations to genes such as BRCA2 should impact approaches to prostate cancer detection and management. As part of these efforts, we have opened the Prostate Cancer Risk Clinic at the University of Michigan and launched a biomarker-driven clinical trial for early prostate cancer detection in men predisposed to aggressive prostate cancer. Emblematic of bringing laboratory insights into the clinic, we have developed a new paradigm for assessing novel biomarkers in the clinical setting by designing and leading the first biomarker-driven randomized controlled trial in this space. Termed the Genomics in Michigan ImpactiNg Observation or Radiation (G-MINOR) trial, this study recently completed enrollment of 350 patients across 13 sites. The trial is designed to test the impact of the Decipher molecular classifier compared to use of a clinical nomogram (CAPRA-S) and will report on the impact of gene expression classifier testing on treatment decisions and cancer control. This trial should help to establish the role of prospective, randomized trial design for biomarker validation in prostate cancer.

2) What was the impact on other disciplines?

Nothing to report

3) What was the impact on technology transfer?

Nothing to report

4) What was the impact on society beyond science and technology?

Nothing to report

Changes/Problems

1) Changes in approach and reasons for change

Continued emphasis on CTC analyses over DTC analyses due to better accrual of blood samples compared to bone marrow aspirates. Development of novel methods for DTC identification.

2) Actual or anticipated problems or delays and actions or plans to resolve them

Nothing to report

3) Changes that had a significant impact on expenditures

Nothing to report

4) Significant changes in use or care of human subjects, vertebrate animals, biohazards, and/or select agents

Nothing to report

5) Significant changes in use or care of human subjects

Nothing to report

6) Significant changes in use or care of vertebrate animals.

Nothing to report

7) Significant changes in use of biohazards and/or select agents

Nothing to report

Products

Publications:

Gogoi P, Sepehri S, Zhou Y, Gorin MA, Paolillo C, Capoluongo E, Gleason K, Payne A, Boniface B, Cristofanilli M, **Morgan TM**, Fortina P, Pienta KJ, Handique K, Wang Y: Development of an Automated and Sensitive Microfluidic Device for Capturing and Characterizing Circulating Tumor Cells (CTCs) from Clinical Blood Samples. PLoS One 11(1): e0147400, 2016.

Qiao Y, Feng FY, Wang Y, Cao X, Han S, Wilder-Romans K, Navone NM, Logothetis C, Taichman RS, Keller ET, Palapattu GS, Alva AS, Smith DC, Tomlins SA, Chinnaiyan AM, **Morgan TM**: Mechanistic Support for Combined MET and AR Blockade in Castration-Resistant Prostate Cancer. Neoplasia 18(1): 1-9, 2016.

Cole AI, **Morgan TM**, Spratt DE, Palapattu GS, He C, Tomlins SA, Weizer AZ, Feng FY, Wu A, Siddiqui J, Chinnaiyan AM, Montgomery JS, Kunju LP, Miller DC, Hollenbeck BK, Wei JT, Mehra R: Prognostic value of percent Gleason grade 4 at prostate biopsy on predicting prostatectomy pathology and recurrence. J Urol 196: 405-11, 2016.

Kozminski MA, Tomlins S, Cole A, Singhal U, Lu L, Skolarus TA, Palapattu GS, Montgomery JS, Weizer AZ, Mehra R, Hollenbeck BK, Miller DC, He C, Feng FY, **Morgan TM**: Standardizing the definition of adverse pathology for lower risk men undergoing radical prostatectomy. Urol Oncol: 2016.

Morgan TM, Hawken SR, Ghani KR, Miller DC, Feng FY, Linsell SM, Salisz JA, Gao Y, Montie JE, Cher ML: Variation in the use of postoperative radiotherapy among high-risk patients following radical prostatectomy. Prostate Cancer Prostatic Dis: 2016.

Palapattu GS, Salami SS, Cani AK, Hovelson DH, Lazo de la Vega L, Vandenberg KR, Bratley JV, Liu CJ, Kunju LP, Montgomery JS, Morgan TM, Natarajan S, Huang J, Tomlins SA, Marks LS: Molecular Profiling to Determine Clonality of Serial Magnetic Resonance Imaging/Ultrasound Fusion Biopsies from Men on Active Surveillance for Low-Risk Prostate Cancer. Clin Cancer Res 23(4): 985-991, 2016. PM28031426

Turner RM 2nd, Morgan TM, Jacobs BL: Epidemiology of the Small Renal Mass and the Treatment Disconnect Phenomenon. Urol Clin North Am 44(2): 147-154, 2017. PM28411907/PMC5407311

Roca H, Jones JD, Purica MC, Weidner S, Koh AJ, Kuo R, Wilkinson JE, Wang Y, Daignault-Newton S, Pienta KJ, **Morgan TM**, Keller ET, Nör JE, Shea LD, McCauley LK: Apoptosis-induced CXCL5 accelerates inflammation and growth of prostate tumor metastases in bone. J Clin Invest: 2018. PM29202471

Patnaik A, Swanson KD, Csizmadia E, Solanki A, Landon-Brace N, Gehring MP, Helenius K, Olson BM, Pyzer AR, Wang LC, Elemento O, Novak J, Thornley TB, Asara JM, Montaser L, Timmons JJ, **Morgan TM**, Wang Y, Levantini E11, Clohessy JG, Kelly K, Pandolfi PP, Rosenblatt JM, Avigan DE, Ye H, Karp JM, Signoretti, S, Balk SP, Cantley LC: Cabozantinib Eradicates Advanced Murine Prostate Cancer by Activating Anti-Tumor Innate Immunity. Cancer Discov 8: 1158/2159-8290, 2017. PM28274958

Hovelson DH, Liu CJ, Wang Y, Kang Q, Henderson J, Gursky A, Brockman S, Ramnath N, Krauss JC, Talpaz M, Kandarpa M, Chugh R, Tuck M, Herman K, Grasso CS, Quist MJ, Feng FY, Haakenson C, Langmore J, Kamberov E, Tesmer T, Husain H, Lonigro RJ, Robinson D, Smith DC, Alva AS, Hussain MH, Chinnaiyan AM, Tewari M, Mills RE, **Morgan TM***, Tomlins SA* (*co-senior authors): Rapid,

ultra low coverage copy number profiling of cell-free DNA as a precision oncology screening strategy. Oncotarget 8(52): 89848- 89866, 2017. PM29163793/PMC5685714

Singhal, U, Wang, Y, Henderson, J, Niknafs, Y, Gursky, A, Zaslavsky, A, Smith, DC, Chang, L, Feng, FY, Palapatu, GS, Taichman, RS, Chinnaiyan, A, Tomlins, S, **Morgan, TM**: Multigene profiling of a circulating tumor cells in mCRPC identifies clinically relevant prognostic signature, Multigene profiling of CTCs in mCRPC identifies a clinically relevant prognostic signature. Mol Cancer Res 16(4): 643-654, 2018. PM29453313

Jung Y, Cackowski FC, Yumoto K, Decker A, Wang J, Kim J, Lee E, Wang Y, Chung JS, Gursky AM, Krebsbach PH, Pienta KJ, **Morgan TM**, Taichman RS: CXCL12γ Promotes Development of Metastatic Castration Resistant Prostate Cancer by Induction of Cancer Stem Cell and Neuroendocrine Phenotypes. Cancer Res 78: 2026-2039, 2018. PM29431639

Kozminsky, M, Fouladdel, S, Chung, J-S, Wang, Y, Smith, D.C., Alva, A, Azizi, E, **Morgan, T.M.***, Nagrath, S.* (*co-senior authors), Detection of CTC Clusters and a Dedifferentiated RNA-Expression Survival Signature in Prostate, Advanced Science 6(2): 1801254, 2018. PMC6343066

Presentations/abstracts:

- Initial Management and Imaging of Advanced Prostate Cancer, AUA, May 2018, San Francisco
- Genetic Testing in Prostate Cancer: Understanding Clinical Implications for Early Detection, Localized Disease & CRPC- Course Director, American Urologic Association, May 2018, San Francisco
- Singhal, U., Wang, Y., Reichert, Z., Tomlins, S., **Morgan, T**.: MP87-03 TARGETED GENE EXPRESSION PROFILING WITHIN CIRCULATING TUMOR CELLS IN MCRPC, American Urological Association, San Francisco, 2018.
- **Morgan, T.M**., Singhal, U., Wang, Y., Henderson, J.: Identification of a CTC-based prognostic signature in mCRPC driven by Aurora Kinase A and Wnt signaling, European Association of Urology, London, 2017.
- Chung, J.S., Wang, Y., Henderson, J., **Morgan, T.M.**,: GAS6, KLK2, and BMP7 detected in circulationg tumor cells predict resistance to chemotherapy in MCRPC, The Journal of Urology, 197, 4S, 1358, 2017.
- **Morgan, TM**: Castration-Resistant Prostate Cancer Live Forum, American Urological Association, Boston, MA, 2017.
- Adams, M., Henderson, J., Lee, M., **Morgan, T.M.**, Palapattu, G.: The Biological ramifications of prostate cancer associated cell free DNA: Effect on platelet function and disease progression, American Urological Association, Boston, The Journal of Urology, 197, 4, 1168, 2017.
- Chung, JS., Wang, Y., Henderson, J., Singhal, U., **Morgan, T**.**M**,: CTC-Based gene expression for

predicting resistance to abiraterone and enzalutamide in MCRPC, American Urologic Association Annual Conference, Boston, The Journal of Urology, 197, 4, 1357, 2017.

- **Morgan, TM**; Chung JS; Wang Y; Henderson J; Singhal U; Qiao Y; Zaslavsky A;: Indentification of a CTC- based gene expression signature predicting resistance to abiraterone and enzalutamide in mCRPC., ASCO, Chicago, 2017.

- Salami SS, Singhal U, Spratt DE, Palapattu GS, Hollenbeck B, Graf R, Louw J, Jendrisak A, Dugan L, Wang Y, Dittamore R, Feng FY, **Morgan TM**: Prevalence and prognostic significance of circulating tumor cells (CTC) in clinically localized prostate cancer, Society of Urologic Oncology Conference, San Antonio, TX, 2016.

- Advanced Prostate Cancer Therapy – Role of the Urologist CME on the Fly- Denver, CO

Participants and Other Collaborating Organizations

1) What individuals have worked on the project?

Name	Yugang Wang
Project Role	Research scientist
Person month worked	3
Contribution	Work on cell line experiments and processing of clinical samples
Funding	Taubman Institute Funding and Prostate Cancer Foundation

Name	Amy Kasputis
Project Role	Clinical Research coordinator
Person month worked	2
Contribution	Work on patient recruitment, sample acquisition, database tracking
Funding	Myriad Genetics, Inc

Name	Yuanyuan Qiao
Project Role	Post-doc
Person month worked	1
Contribution	Work on cell line experiments
Funding	Chinnaiyan lab, NIH

Name	Huiru Zhao
Project Role	Post-doc
Person month worked	5
Contribution	Analysis of clinical samples
Funding	Taubman Institute

2) Changes in active other support:

There was no change in the PI's effort on this award. Other support is as follows:

16-PAF04514 (Lin) 12/01/2016-11/30/2021
NIH
Title: Prostate cancer Active Surveillance Study (PASS)
Goals: Continued to enrolment and follow-up for participants in the Canary Prostate Active Surveillance Study (PASS) Protocol, open for enrollment at University of Michigan since May, 2010.
Role: site PI

1-R01-CA-193331-01-A1 (Victorson) 09/01/2015-08/31/2020
NIH
Title: REASSURE ME trial
Goals: examine the efficacy of an 8-week mindfulness based stress reduction course for men diagnosed with prostate cancer on active surveillance and their spouses
Role: site PI

2-P01-CA093900-11A1 (Keller) 10/01/2015-09/30/2020
NIH
Title: The Biology of Prostate Cancer Skeletal Metastases
Goals: The ultimate goal is to define the cellular and molecular mechanisms that surround PCa skeletal metastases to facilitate translation into clinical application
Role: Co-I

MDxHealth, Inc. (Morgan) 12/01/2016-05/31/2019
Title: Prospective Validation of Prostate Biomarkers for Repeat Biopsy: The PRIORITY Study
Goals: This multi-institutional prospective trial is designed to assess the clinical validity of the ConfirmMDx tissue-based biomarker in men with a previous negative prostate biopsy who are undergoing repeat biopsy.
Role: PI

16-PAF08152 (Morgan) 12/01/2016-11/30/2018
MDxHealth
Title: Targeted Early Detection Program in Men at High Genetic Risk for Prostate Cancer
Goals: This is a prospective study of men with increased genetic risk of prostate cancer (eg BRCA1, BRCA2, Lynch syndrome), assessing the impact of a dedicated early detection program.
Role: PI

Emerging Scholar Award (Morgan) 01/2015-12/2018
A. Alfred Taubman Medical Institute
Title: Liquid biopsy in advanced prostate cancer
Goals: Identify mechanisms of resistance in advanced prostate cancer through transcriptional profiling of circulating tumor cells in men with metastatic castration resistant prostate cancer.
Role: PI

Blue Boxer Award (Morgan) 07/2018-06/2019
Title: Evaluation of a Streamlined Approach to Genetic Testing in Localized and Advanced Prostate Cancer
Goals: Develop an oncologist-driven genetic testing approach for men with prostate cancer and determine patient satisfaction with this streamlined testing model.
Role: PI